Magnetic Circular Dichroism of $[Cr(CN)_5NO]^{3-}$

Hiroshi KOBAYASHI, Ken EGUCHI, and Youkoh KAIZU

Department of Chemistry, Tokyo Institute of Technology, Ookayama, Meguro-ku, Tokyo 152

(Received July 27, 1974)

Magnetic circular dichroism (MCD) was observed in the region of the 22000 cm^{-1} band of $[Cr(CN)_5NO]^{3-}$. The absorption band was assigned to a charge-transfer transition linearly polarized in the direction of Cr–NO, while the MCD observed in the same region was assigned to B term extrema of the (d, d*) transitions hidden beneath the charge-transfer band. The charge-transfer transition gives rise to an absorption peak but no MCD, since the transition is polarized in the direction of the orbital angular momentum, even in the case where a degenerate excited state is involved.

The electronic structure of $[M(CN)_5NO]^{n-}$ complexes has been established on the basis of magnetic, spectroscopic and theoretical studies.[1–15] The weight of evidence shows a strong M–NO π-bonding.[16–21] However the important role of the π^*_{NO} orbital in the low-energy excitations had not been considered until Manoharan and Gray interpreted the electronic excitations of $[M(CN)_5NO]^{n-}$ in terms of self-consistent charge and configuration-molecular orbital (SCCC MO) calculations.[20]

According to the most recent suggestion,[22] the order of the orbitals responsible for the outer electronic configuration is: $1e<xy<2e<x^2-y^2<z^2$, where xy, x^2-y^2, and z^2 denote the molecular orbitals predominantly distributed on the metal d_{xy}, $d_{x^2-y^2}$, and d_{z^2} orbitals, and 1e and 2e are the highest occupied and the lowest vacant degenerate orbital pairs, which are mainly composed of metal d_{zx} and d_{yz} orbitals and the lowest nitric oxide antibonding π orbitals $\pi_x^*{}_{NO}$ and $\pi_y^*{}_{NO}$.

The ESR data for $[CrL_5NO]$ (L: CN^-, NH_3, OH_2) have been interpreted for the ground electronic configuration $(1e)^4(xy)$.[20,23,24] The unpaired electron relevant to an almost isotropic ESR signal is localized predominantly in the d_{xy} orbital. A characteristic absorption band observed around 22000 cm^{-1} is fairly constant both in position and intensity for L=CN^-, NH_3, H_2O and C_2H_5OH in $[CrL_5NO]$,[25] and has been assigned to the transition $^2B_2 \rightarrow {}^2B_2$ ($(1e)^4(xy) \rightarrow (1e)^3(2e)(xy)$) which is linearly polarized in the direction of the Cr–NO bond.[20] In the present work, however, magnetic circular dichroism (MCD) was observed in the region of the 22000 cm^{-1} band of $[CrL_5NO]$.

Experimental

$K_3[Cr(CN)_5NO]\cdot H_2O$ was prepared by the method described in the literature.[26] The sample was recrystallized twice from water. The bright green crystals thus obtained were identified by elemental analysis.

Found: C, 17.2; H, 0.4; N, 24.5; Cr, 15.0%. Calcd for $K_3[Cr(CN)_5NO]\cdot H_2O$: C, 16.7; H, 0.6; N, 24.2; Cr, 15.0%.

$[Cr(NH_3)_5NO]Cl_2$ was prepared and purified by the method of Mori, Ueshiba and Kawaguchi.[27] The brown crystals thus obtained were identified by analysis for chromium.

Found: Cr, 22.1%. Calcd for $[Cr(NH_3)_5NO]Cl_2$: Cr, 21.8%.

A perchloric acid solution of $[Cr(OH_2)_5NO](ClO_4)_2$ was prepared by the method described in the literature.[25]

Our MCD measurement technique has been described elsewhere.[28] All the measurements were carried out on a JASCO Model ORD/UV-5 instrument with its electromagnet. The magnetic field was set at 10000 G The electronic absorption spectra of solutions and films were taken on a Shimadzu automatic recording spectrophotometer Model MPS-50. The instruments were furnished with a Dewar for low-temperature measurement. The polarizing microscope absorption spectrum of a single crystal was taken by courtesy of Professors Kondo and Nakahara, St. Paul's University, on a Hitachi automatic recording spectrophotometer Model EPS-3T equipped with a special microscope. A single crystal suitable for the measurement was selected on a polarizing microscope from crystals deposited on a clean glass plate by the spontaneous evaporation of an aqueous solution of $K_3[Cr(CN)_5NO]$. The extinction axis of the crystal was coincident with the direction of growth of the crystal needles (c axis).

The magnitude of MCD is reported here in terms of molar circular dichroism per unit external magnetic field, $(\varepsilon_l-\varepsilon_r)/H_z$, where ε_l and ε_r represent the molar absorption coefficients for left and right circularly polarized light, respectively, and H_z is the strength of external magnetic field.

The magnitude of molar circular dichroism per unit external magnetic field observed at a transition a→j is given by

$$(\varepsilon_l-\varepsilon_r)/H_z = -\left(\frac{16\pi}{3hc}\right)\frac{N}{10^3 \ln 10}\{f_1 A + f_2(B+C/kT)\},$$

where the function f_1 is a shape function of the sigmoidal dispersion at the position of the absorption maximum ν_{ja}, the function f_2 is a shape function as approximated by a Gaussian with an extremum at the absorption maximum.[29–21]

The MCD and absorption spectra were measured with $[Cr(OH_2)_5NO]^{2+}$ in concd $HClO_4$ solution, $[Cr(NH_3)_5NO]^{2+}$ in 0.1 M HCl solution, and $[Cr(CN)_5NO]^{3-}$ in aqueous solution, in 2 : 1 mixture of propyleneglycol and water, and in a polyvinyl alcohol (PVA) film. The 2 : 1 mixture of propyleneglycol and water gave a transparent rigid glass dispersing an electrolyte such as $K_3[Cr(CN)_5NO]$ down to dry ice–methanol temperature (195 K). However the transparence of the rigid glass in the near-ultraviolet region became poor at dry ice–methanol temperature. The MCD spectrum of $[Cr(CN)_5NO]^{3-}$ in a PVA film was obtained at various temperatures down to liquid nitrogen temperature. A PVA film was made by spontaneous evaporation of an aqueous solution of PVA on a glass plate and then the film was heated up to 90 °C for 1 hr in order to increase its transparence. A transparent PVA film thus obtained was swelled a little in water and then dyed in an aqueous solution of $K_3[Cr(CN)_5NO]$. The dyed film was dried at room temperature for 24 hr over phosphorous pentoxide under reduced pressure. The spectrum of this yellow ochreous transparent film was in good agreement with the solution spectrum.

Results and Discussion

The visible and near-ultraviolet MCD and absorption spectra of $[Cr(CN)_5NO]^{3-}$ in aqueous solution and in a 2 : 1 mixture of propyleneglycol and water are shown in Fig. 1. The MCD and absorption spectra around 22000 cm^{-1} of $[Cr(CN)_5NO]^{3-}$ in PVA film were also measured at various temperatures down to liquid nitrogen temperature. The result is shown in Fig. 2.

An apparent dispersion of MCD was observed at 23700 cm^{-1}. An MCD maximum corresponds to the absorption peak at 22100 cm^{-1}, whereas no absorption maximum was observed corresponding to the MCD minimum at 25400 cm^{-1}. $[Cr(NH_3)_5NO]^{2+}$ and $[Cr(OH_2)_5NO]^{2+}$ also show a similar absorption band

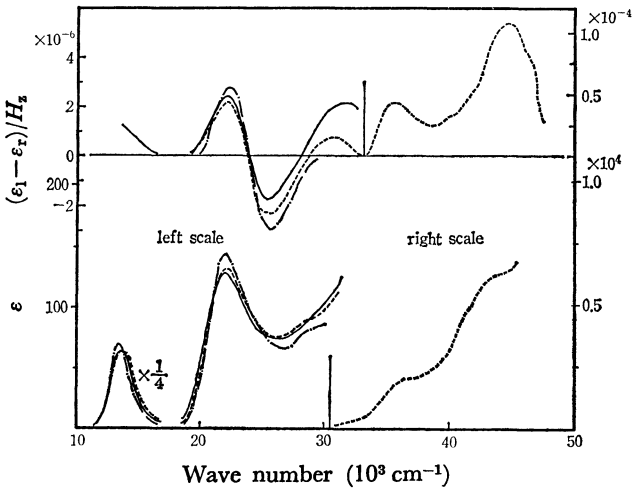

Fig. 1. Magnetic circular dichroism and absorption spectra of $[Cr(CN)_5NO]^{3-}$.
----: in 2 : 1 mixture of propyleneglycol and water (at 300 K), -·-·-: in 2 : 1 mixture of propyleneglycol and water (at 195 K), ——: in aqueous solution.

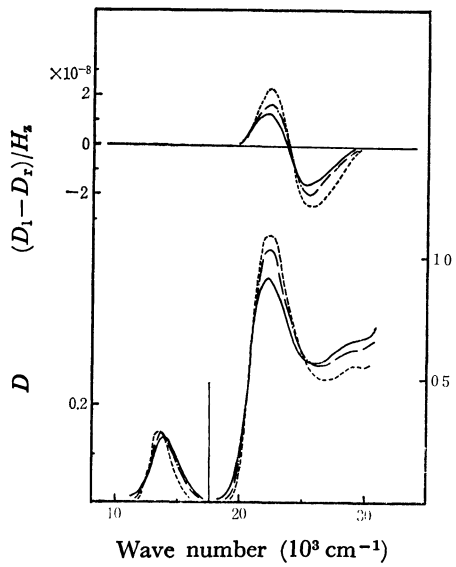

Fig. 2. Magnetic circular dichroism and absorption spectra of $[Cr(CN)_5NO]^{3-}$ on polyvinyl alcohol film. ——: at 300 K, -·-·-: at 195 K, ----: at 77 K.

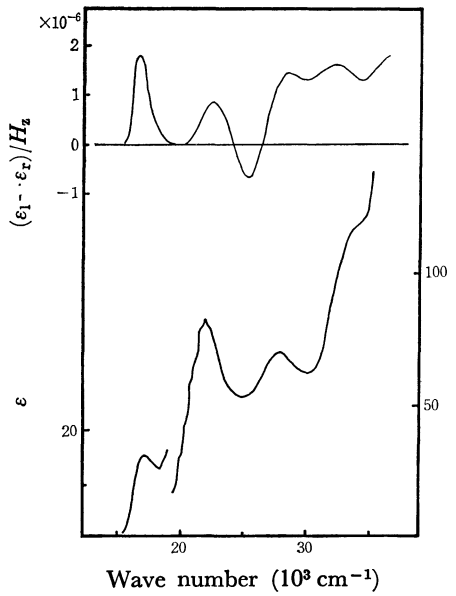

Fig. 3. Magnetic circular dichroism and absorption spectra of $[Cr(NH_3)_5NO]^{2+}$ in 0.1 M HCl solution.

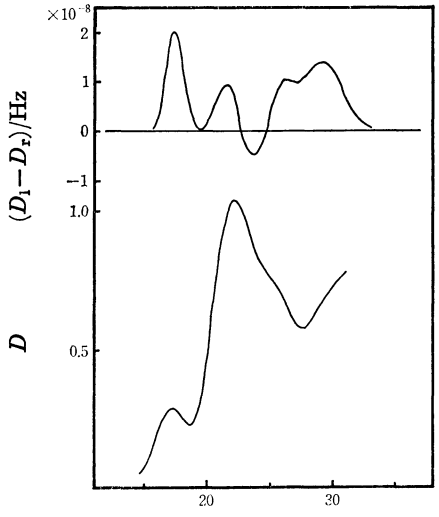

Fig. 4. Magnetic circular dichroism and absorption spectra of $[Cr(OH_2)_5NO]^{2+}$ in concd $HClO_4$ solution.

around 22000 cm^{-1}, and their MCD extrema are also not coincident with their absorption maxima. The substitution of L in $[CrL_5NO]$ gives rise to a small but detectable shift of the 22000 cm^{-1} absorption maximum in the opposite direction to the shift of the MCD maximum. The MCD and absorption spectra of $[Cr(NH_3)_5NO]^{2+}$ in 0.1 M HCl solution and of $[Cr(OH_2)_5NO]^{2+}$ in concd $HClO_4$ solution are shown in Figs. 3 and 4 although the spectra of the latter are rather qualitative. The whole profile of the MCD spectra of $[Cr(NH_3)_5NO]^{2+}$ and $[Cr(OH_2)_5NO]^{2+}$ is similar to that of $[Cr(CN)_5NO]^{3-}$. It should be noted that the lowest energy MCD peak and its corresponding absorption maximum (at about 22000 cm^{-1}) show a shift opposite to the spectrochemical series upon substitution of L in $[CrL_5NO]$ whereas the other MCD extrema show a shift coincident with the spectrochem-

Table 1. The magnetic circular dichroism extrema and absorption maxima of the chromium nitrosyl complexes

Complex	Absorption maxima (10^3 cm^{-1})					MCD extrema (10^3 cm^{-1})				
	I	II	III	IV	V	I	II	III	IV	V
$[Cr(CN)_5NO]^{3-}$	13.7	22.2		28.6			22.1	25.6	30.4	
$[Cr(NH_3)_5NO]^{2+}$	17.1	21.9		27.8	33.4	16.6	22.4	25.2	28.4	32.2
$[Cr(OH_2)_5NO]^{2+}$	17.4	22.2		25.8		17.4	21.6	23.7	25.2	29.0

ical series. The observed MCD extrema are summarized in Table 1. The 22000 cm^{-1} band of $[Cr(CN)_5NO]^{3-}$ in PVA does not show ripple structure even at 77 K, although the single crystal absorption spectrum at room temperature shows a trace of ripple structure. The corresponding band of $[Cr(NH_3)_5NO]^{2+}$, however, displays a remarkable ripple structure in 0.1 M HCl solution even at room temperature. On the other hand, the MCD spectrum of $[Cr(NH_3)_5NO]^{2+}$ around 22000 cm^{-1} does not show any indication of vibrational fine structure. The differences observed in the behavior of the MCD and absorption spectra around 22000 cm^{-1} indicate that MCD measurements can detect a ligand-field (d, d*) transition hidden in a characteristic absorption band arising from the charge-transfer transition 1e→2e in Cr–NO. This charge-transfer band is rather independent of the other ligands present in the complexes.

Since the molecular orbital pairs, both 1e and 2e, have a z component of orbital angular momentum $\Lambda_z=\pm1$, the charge-transfer excitation 1e→2e gives rise to $^2\Delta$ ($\Lambda_z=\pm2$) and $^2\Sigma$ ($\Lambda_z=0$) states. A transition from the ground $^2\Sigma$ state to the excited $^2\Sigma$ state is allowed, whereas the one to the excited $^2\Delta$ state is forbidden. The molar absorption coefficient of the band around 22000 cm^{-1} is about 130 in $[Cr(CN)_5NO]^{3-}$. If this band arises from a charge-transfer transition in Cr–NO, it should be assigned to a forbidden transition, $^2\Sigma\rightarrow{}^2\Delta$. The forbidden transition can borrow spectral intensity from the allowed transition $^2\Sigma\rightarrow{}^2\Sigma$ by a degenerate vibration which removes the degeneracy of the molecular orbital pairs and gives rise to a mixing between allowed and forbidden transitions. The participating vibration is either a degenerate bending vibration of the Cr–NO skeleton or, less possibly, a degenerate stretching vibration of the Cr–$(CN)_4$ skeleton in a plane perpendicular to the Cr–NO axis. In fact, a vibrational progression has been found on the low-energy side of the 22000 cm^{-1} band of $[(n\text{-}C_4H_9)_4N]_3[Cr(CN)_5NO]$ in EPA solution at 100 K.[20] The band around 22000 cm^{-1} in $[Cr(NH_3)_5NO]^{2+}$ is also accompanied by ripples spaced at about 480—490 cm^{-1} intervals. Bernal assumed a contribution of the Cr–$(NH_3)_4$ stretching vibration in a place perpendicular to the Cr–NO bond.[20] Kobayashi, Tsujikawa, Mori, and Yamamoto, suggested participation of the degenerate bending vibration of the Cr–NO skeleton which is observed at 531—535 cm^{-1} in the vibration spectrum.[24] However they assigned the 22000 cm^{-1} band to the ligand-field transition $^2B_2(xy)\rightarrow{}^2B_1(x^2-y^2)$ which should be coupled with a vibration of E symmetry in order to be allowed. Since no similar ripple structure had been found in the (d, d*) transitions of other chromium ammine complexes, a possibility of participation of the degenerate Cr–$(NH_3)_4$ stretching mode was eliminated. If the 22000 cm^{-1} band arises from a forbidden charge-transfer transition $^2\Sigma\rightarrow{}^2\Delta$ in Cr–NO, the transition can borrow intensity from the allowed $^2\Sigma\rightarrow{}^2\Sigma$ transition, coupled either with a degenerate bending vibration of the Cr–NO skeleton or much less possibly, with a degenerate stretching vibration in the Cr–$(NH_3)_4$ skeleton. In the case of $[Cr(NH_3)_5NO]^{2+}$ the bond between chromium and coordinated NH_3 has the nature of a σ coordination bond, whereas in the case of $[Cr(CN)_5NO]^{3-}$ the back-bonding character of the chromium–CN^- bond is appreciable. Thus, in $[Cr(CN)_5NO]^{3-}$, a small participation of the stretching vibration cannot always be eliminated.

The fact that the position of the 22000 cm^{-1} band is rather independent of other ligands present in the complex and the band has a ripple structure indicates a transition mainly localized in the Cr–NO bond. The charge-transfer excitations in Cr–NO, both allowed and forbidden, are polarized in the direction of the Cr–NO bond and do not have any appreciable transition dipole in the plane perpendicular to the bond axis. It was experimentally proved that a similar forbidden charge-transfer transition in $Na_2[Fe(CN)_5NO]$ is polarized in the direction of the Fe–NO bond.[20] Since a linear oscillator collinear with the orbital angular momentum shows no Zeeman splitting, a charge-transfer transition linearly polarized in the direction of the Cr–NO bond does not display any MCD.

A schematic energy diagram of the orbitals responsible for the outer electronic configuration is shown in Fig. 5. The order of orbitals $a_1(z^2)$ and $b_1(x^2-y^2)$ depends upon σ donations from coordinated NO^+ and CN^-, NH_3 or OH_2. The bonding molecular orbital pair 1e is appreciably lower than orbital $b_2(xy)$ for a π-bonding interaction between metal $d\pi$ orbitals

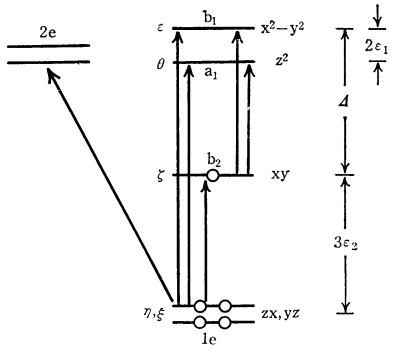

Fig. 5. The energy diagram of the outer shell electrons (schematic).

TABLE 2. THE LOWEST LIGAND-FIELD (d, d*) EXCITED DOUBLETS

Excited doublets	Diagonal energy
$^2B_1(1e^4b_1)$ $\|\varepsilon\xi\bar{\xi}\eta\bar{\eta}\|$	Δ
$^2A_1(1e^4a_1)$ $\|\theta\xi\bar{\xi}\eta\bar{\eta}\|$	$\Delta - 2\varepsilon_1 + 20kB$
$1^2E_0(1e^3b_2^2)$[a] $\|\xi\zeta\bar{\zeta}\eta\bar{\eta}\|$	$3\varepsilon_2 + (16-3k+13k^2)B$
$2^2E_0(1e^3b_2a_1)$[a] $[\|\theta\zeta\bar{\xi}\eta\bar{\eta}\| - \|\theta\zeta\bar{\xi}\eta\bar{\eta}\|]/\sqrt{2}$	$\Delta + 3\varepsilon_2 - 2\varepsilon_1 + (-8+45k-26k^2)B/2$
$3^2E_0(1e^3b_2b_1)$[a] $[2\|\bar{\varepsilon}\zeta\bar{\xi}\eta\bar{\eta}\| - \|\varepsilon\bar{\zeta}\bar{\xi}\eta\bar{\eta}\| - \|\varepsilon\zeta\bar{\xi}\eta\bar{\eta}\|]/\sqrt{6}$	$\Delta + 3\varepsilon_2 + (20+k-26k^2)B/2$
$4^2E_0(1e^3b_2b_1)$[a] $[\|\varepsilon\bar{\zeta}\bar{\xi}\eta\bar{\eta}\| - \|\varepsilon\zeta\bar{\xi}\eta\bar{\eta}\|]/\sqrt{2}$	$\Delta + 3\varepsilon_2 + (12+15k-26k^2)B/2$
$5^2E_0(1e^3b_2a_1)$[a] $[2\|\bar{\theta}\zeta\bar{\xi}\eta\bar{\eta}\| - \|\theta\bar{\zeta}\bar{\xi}\eta\bar{\eta}\| - \|\theta\zeta\bar{\xi}\eta\bar{\eta}\|]/\sqrt{6}$	$\Delta + 3\varepsilon_2 - 2\varepsilon_1 + (8+27k-26k^2)B/2$
Non-zero mixing term	**energy**
$<2^2E_0\|\hat{H}\|3^2E_0>$	$-1.5\,kB$
$<2^2E_0\|\hat{H}\|4^2E_0>$	$-2.5\sqrt{3}\,kB$
$<2^2E_0\|\hat{H}\|5^2E_0>$	$\frac{1}{\sqrt{12}}(15k-24)B$
$<3^2E_0\|\hat{H}\|4^2E_0>$	$\frac{1}{\sqrt{12}}(21k-12)B$
$<3^2E_0\|\hat{H}\|5^2E_0>$	$-3.5\sqrt{3}\,kB$
$<4^2E_0\|\hat{H}\|5^2E_0>$	$-1.5\,kB$

a) For the degenarate states, only one component of the wave functions is given.

zx and yz and NO antibonding orbitals π^*_{NO}. As ESR studies show, the ground state should be a ^2B state with electronic configuration $(1e)^4(b_2)$. The energy of the lowest one-electron excited doublets is obtained in terms of orbital energy parameters Δ, ε_1, and ε_2 and Racah's electrostatic parameter B as in Table 2. An empirical relationship $C=4.0B$ was assumed and the value of B was reduced for the delocalization in molecular orbital 1e following Koide and Pryce:[32] $B(e,e)=k^2B$, $B(e,b_2)=kB$, and $B(b_2,b_1)=B$.

The empirical values of Δ are 13900 cm^{-1} in $[Cr(OH_2)_6]^{2+}$ and 17400 cm^{-1} in $[Cr(OH_2)_6]^{3+}$.[33] Since the formal oxidation state of chromium in $[Cr(OH_2)_5NO]^{2+}$ is 1+, the value of Δ should be less than 13900 cm^{-1}. Furthermore an almost isotropic ESR signal indicates a large energy gap between 1e and b_2. The energies of ligand-field excited doublets were calculated for a variety of parameters Δ, ε_1, ε_2 in units of B. The lowest observed ligand-field bands in $[Cr(OH_2)_5NO]^{2+}$ and $[Cr(NH_3)_5NO]^{2+}$ are assigned to transitions to excited states $^2A_1$ ($b_2\rightarrow a_1$) and 1^2E ($1e\rightarrow b_2$). The next four ligand-field transitions above 20000 cm^{-1} are assigned to four ^2E states arising from excitations $1e\rightarrow b_1$ and $1e\rightarrow a_1$. In the case of $[Cr(CN)_5NO]^{3-}$, an increase in Δ gives rise to a blue-shift of the transitions to $^2B_1(b_2\rightarrow b_1)$ and to $^2A_1(b_2\rightarrow a_1)$. The back-bonding interactions of coordinated CN^- push down orbital b_2. This reduces the value of ε_2 and gives rise to a red-shift of the transition to $1^2E(1e\rightarrow b_2)$. As shown in Figs. 3 and 4, a red absorption band and its closely corresponding MCD maximum are observed in $[Cr(NH_3)_5NO]^{2+}$ and $[Cr(OH_2)_5NO]^{2+}$. Because insufficient sensitivity of our instrument, the MCD maximum of $[Cr(CN)_5NO]^{3-}$ in near-infrared region could not be detected. An MCD maximum, however, is expected at 13700 cm^{-1} corresponding to the absorption peak (Fig. 1). The lowest wave number band is red-shifted in the order

$$[Cr(CN)_5NO]^{3-} > [Cr(NH_3)_5NO]^{2+} > [Cr(OH_2)_5NO]^{2+}.$$
(13700 cm^{-1}) (17100 cm^{-1}) (17400 cm^{-1})

The absorption intensity of the lowest wave number band of $[Cr(NH_3)_5NO]X_2$ depends upon the outer sphere anions in the complex salts: the color of the complex salts varies from brown to green. Thus Kobayashi, Tsujikawa, Mori and Yamamoto have assigned the lowest wave number band to a charge-transfer excitation in the Cr–NO bond.[24] The observations in the present work, however, indicate that the red absorption band should be assigned to a (d, d*) transition rather than a charge-transfer transition. The red absorption band, however, should have two components corresponding to $^2B_1(b_2\rightarrow b_1)$ and $1^2E(1e\rightarrow b_2)$. In fact, the single crystal absorption spectrum of $K_3[Cr(CN)_5NO]\cdot H_2O$ exhibits two different peaks in the red band for polarized light $\parallel$ and $\perp$ to the c axis as shown in Fig. 6. The spectra polarized $\parallel$ and $\perp$ to the optically equivalent Cr–NO axis could not be obtained because of the crystal disorder, which had been revealed by X-ray crystallography.[34] Since the 22000 cm^{-1} absorption is linearly polarized along the Cr–NO axis, the fact that the absorption for the light polarized $\parallel$ to the c axis is a little more intense than that for the light polarized $\perp$ to the c axis indicates that a slightly higher number of complexes have their Cr–NO bonds $\parallel$ to the c axis. Thus the lower wavenumber component of the red absorption band (680 nm, 14700 cm^{-1}) is polarized more $\parallel$ to the Cr–NO axis and the higher wave number component (670 nm, 14900 cm^{-1}) is polarized more $\perp$ to the Cr–NO axis.

The excited states n^2E arising from the excitations $1e\rightarrow b_1$ and $1e\rightarrow a_1$ in $[Cr(CN)_5NO]^{3-}$ correspond well to

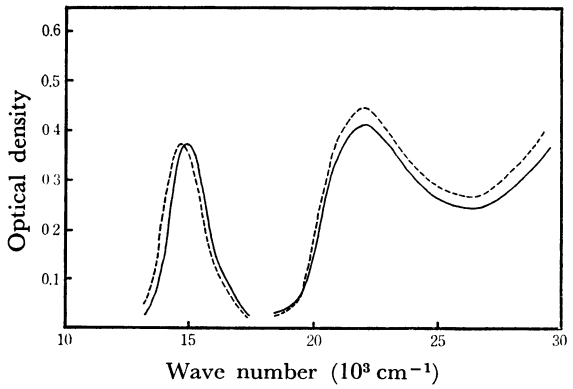

Fig. 6. The polarized single crystal absorption spectrum of $K_3[Cr(CN)_5NO]\cdot H_2O$.
——: polarized $\perp$ to c axis
----: polarized $\parallel$ to c axis

those in $[Cr(NH_3)_5NO]^{2+}$ and $[Cr(H_2O)_5NO]^{2+}$. The calculated energy of the lowest excited doublets is shown in Fig. 7. For a reasonable choice of parameters, theory can reproduce the ligand-field (d, d*) excited states which were detected by MCD spectra as in Fig. 8. The same parameters also predict that the ground state of $[CrL_5NO]$ is ^2B rather than ^6A, and that 1^4E arising from configurations $(1e)^3b_2b_1$ in $[Cr(CN)_5NO]^{3-}$ is higher than 1^2E, which arises from configuration $(1e)^3b_2^2$, whereas 1^4E is lower than 1^2E in $[Cr(NH_3)_5NO]^{2+}$ and $[Cr(OH_2)_5NO]^{2+}$. In fact, the anisotropy of the g value for $[Cr(CN)_5NO]^{3-}$ is different from that of $[Cr(NH_3)_5NO]^{2+}$ and $[Cr(OH_2)_5NO]^{2+}$, *i.e.* the sign of $\Delta g_\perp$ ($\equiv g_\perp - 2.0023$) is reversed. The g values observed and calculated for $[CrL_5NO]$ are summarized in Table 3. The g values are given within

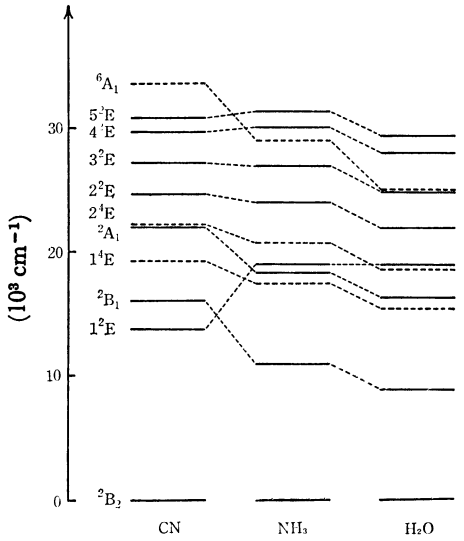

Fig. 7. The lowest ligand-field excited doublets in $[CrL_5NO]$ (L=CN$^-$, NH_3, OH_2).
L=CN$^-$ $\Delta=16{,}000$ cm^{-1}, $\varepsilon_1=500$ cm^{-1} $\varepsilon_2=10000/3$ cm^{-1}, $B=500$ cm^{-1}, $k=0.7$
L=NH_3 $\Delta=11{,}000$ cm^{-1}, $\varepsilon_1=500$ cm^{-1} $\varepsilon_2=14500/3$ cm^{-1}, $B=600$ cm^{-1}, $k=0.7$
L=OH_2 $\Delta=9{,}000$ cm^{-1}, $\varepsilon_1=500$ cm^{-1} $\varepsilon_2=14500/3$ cm^{-1}, $B=600$ cm^{-1}, $k=0.7$

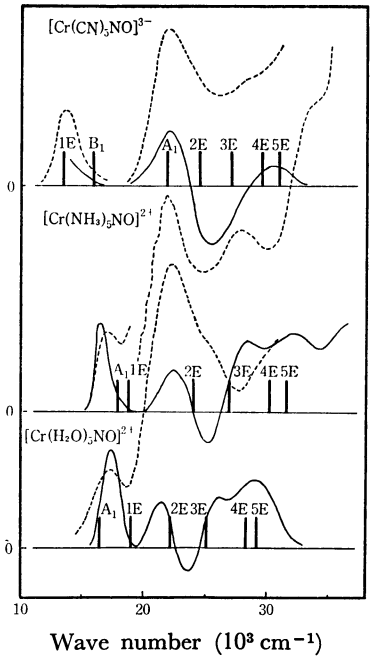

Fig. 8. Assignments of the ligand-field excited states of $[CrL_5NO]$ (L=CN$^-$, NH_3, OH_2).
——: MCD spectrum, ----: absorption spectrum
Vertical lines indicate the calculated energies of the ligand-field excited states.

TABLE 3. THE g VALUES OF $[CrL_5NO]$ (L=CN$^-$, NH_3, OH_2)

L	g obsd			g calcd		
	$g_\parallel$	$g_\perp$	g_{iso}	$g_\parallel$	$g_\perp$	g_{iso}
CN$^-$	1.975	2.005	1.995[a]	1.952	2.004	1.987
NH_3	1.947	1.993	1.980[b]	1.930	1.996	1.974
H_2O	1.916	1.991	1.966[c]	1.913	1.995	1.968

a) Ref 19. b) Estimated from the values for $[Cr(H_2O)_5NO]^{2+}$ (Ref. 35.) c) Ref. 10.

the first-order term of spin-orbit coupling parameter λ as follows:

$$g_\parallel = 2.0023 - 8\lambda/E(^2B_1),$$

$$g_\perp = 2.0023 + 2\lambda/E(1^2E) - \sum_m 2\lambda/E(m^4E_{1/2})\{(1/3)(c_1^m)^2+(c_2^m)^2\} + \sum_n 2\lambda/E(n^2E)\{-(3/2)(c_1^n)^2+(1/3)(c_2^n)^2 - (1/2)(c_3^n)^2 + (c_4^n)^2\},$$

where $E(\Gamma)$ denotes the energy of excitation to state Γ, c_i^m and c_j^n denote the coefficients in the state wave functions

$$\phi(m^4E_{1/2}) = \sum_i c_i^m \phi_i',$$

$$\phi(n^2E) = \sum_j c_j^n \phi_j,$$

$$\phi_1' = \{|\bar{\varepsilon}\zeta\xi\eta\bar{\eta}| + |\varepsilon\bar{\zeta}\xi\eta\bar{\eta}| + |\varepsilon\zeta\bar{\xi}\eta\bar{\eta}|\}/\sqrt{3},$$

$$\phi_2' = \{|\bar{\theta}\zeta\xi\eta\bar{\eta}| + |\theta\bar{\zeta}\xi\eta\bar{\eta}| + |\theta\zeta\bar{\xi}\eta\bar{\eta}|\}/\sqrt{3},$$

$$\phi_1 = \{|\theta\bar{\zeta}\xi\eta\bar{\eta}| - |\theta\zeta\bar{\xi}\eta\bar{\eta}|\}/\sqrt{2},$$

$$\phi_2 = \{2|\bar{\varepsilon}\zeta\xi\eta\bar{\eta}| - \varepsilon\bar{\zeta}\xi\eta\bar{\eta}| - |\varepsilon\zeta\bar{\xi}\eta\bar{\eta}|\}/\sqrt{6}\,,$$

$$\phi_3 = \{|\varepsilon\bar{\zeta}\xi\eta\bar{\eta}| - |\varepsilon\zeta\bar{\xi}\eta\bar{\eta}|\}/\sqrt{2}\,,$$

$$\phi_4 = \{2|\bar{\theta}\zeta\xi\eta\bar{\eta}| - |\theta\bar{\zeta}\xi\eta\bar{\eta}| - |\theta\zeta\bar{\xi}\eta\bar{\eta}|\}/\sqrt{6}\,,$$

and ε, θ, ζ, ξ, and η denote x^2-y^2, z^2, xy, yz, and zx orbitals, respectively. This indicates that $\Delta g_\perp > 0$ when ^1E is higher than $^1{}^2E$ as in $[Cr(CN)_5NO]^{2-}$, whereas $\Delta g_\perp < 0$ when it is lower as in $[Cr(NH_3)_5NO]^{2+}$ and $[Cr(OH_2)_5NO]^{2+}$. The $g_\perp$ value was evaluated assuming $\lambda = 100\ cm^{-1}$ which correctly predicts the value of $g_\parallel$. The delocalization in molecular orbitals reduces the spin-orbit coupling effect in Cr and thus the value of λ in the complex should be smaller than that observed in the atomic spectrum. The calculated values are in good agreement with the observed values. This confirms the assignment of MCD extrema to the ligand-field excitations.

Plots of the ratio of $\int\left(\frac{\varepsilon_l-\varepsilon_r}{H_z}\right)\bar{\nu}\,d\bar{\nu}$ to $\int \varepsilon/\bar{\nu}\,d\bar{\nu}$ against $1/kT$ give a straight line. If an MCD maximum is assumed at 22000 cm^{-1}, apparent values of B/D and C/D in units of transition dipole strength D are obtained as $-0.11\times10^{-3}\beta/cm^{-1}$ and $-0.0059\,\beta$, respectively. Such a relatively temperature-independent MCD is seemingly consistent with the non-degenerate ground state $^2B_2$. These values, however, are less significant in this particular case, where the transition detected by MCD is not the transition detected by absorption in the same wave number region.

The authors would like to thank Dr. Hanako Kobayashi, Kyoto University, and Professor Masayasu Mori, Osaka City University, for more than useful comments. The authors wish to express their appreciation to Professors Yukio Kondo and Masayoshi Nakahara, St. Paul's University, for the measurements of polarizing microscope absorption spectrum. This work was supported by a grant from the Ministry of Education.

References

1) F. A. Cotton, R. R. Monchamp, R. J. M. Henry, and R. C. Young, *J. Inorg. Nucl. Chem.*, **10**, 28 (1959).
2) I. Bernal and S. E. Harrison, *J. Chem. Phys.*, **34**, 102 (1961).
3) C. S. Naiman, *ibid.*, **35**, 1503 (1961).
4) H. B. Gray and C. J. Ballhausen, *ibid.*, **36**, 1151 (1962).
5) I. Bernal and S. E. Harrison, *ibid.*, **38**, 2581 (1963).
6) Y. J. Israeli, *Bull. Soc. Chim. Fr.*, **1964**, 1145.
7) P. T. Manoharan and H. B. Gray, *J. Amer. Chem. Soc.*, **87**, 3340 (1965).
8) H. B. Gray, P. T. Manoharan, J. Pearlman, and R. F. Riley, *Chem. Commun.*, **1965**, 62.
9) H. A. Kuska and M. T. Rogers, *J. Chem. Phys.*, **42**, 3034 (1965).
10) I. Bernal, S. D. Robinson, L. S. Meriwether, and G. Wilkinson, *Chem. Commun.*, **1965**, 571.
11) B. A. Goodman, J. B. Raynor, and M. C. R. Symons, *J. Chem. Soc., A*, **1966**, 994.
12) J. Danon, R. P. A. Muniz, and A. O. Caride, *J. Chem. Phys.*, **46**, 1210 (1967).
13) D. B. Brown, *Inorg. Chim. Acta*, **5**, 314 (1971).
14) P. T. Manobaran, and P. Ganguli, *Chem. Phys. Lett.*, **11**, 281 (1971).
15) L. Tosi, *J. Chim. Phys.*, **69**, 1052 (1972).
16) J. Lewis, R. J. Irving, and G. Wilkinson, *J. Inorg. Nucl. Chem.*, **7**, 32 (1958).
17) P. T. Manoharan and W. C. Hamilton, *Inorg. Chem.*, **2**, 1043 (1963).
18) J. Danon, *J. Chem. Phys.*, **41**, 3378 (1964).
19) J. J. Fortaman and R. G. Hayes, *ibid.*, **43**, 15 (1965).
20) P. T. Manoharan and H. B. Gray, *Inorg. Chem.*, **5**, 823 (1966).
21) G. Paliani and A. Polette., *Spectrosc. Lett.*, **5**, 105 (1972).
22) R. F. Fenske and R. L. DeKock, *Inorg. Chem.*, **11**, 437 (1972).
23) J. Danon, H. Panepucci, and A. A. Misetich, *J. Chem. Phys.*, **44**, 4154 (1966).
24) H. Kobayashi, I. Tsujikawa, M. Mori, and Y. Yamamoto, This Bulletin, **42**, 709 (1969).
25) W. P. Griffith, *J. Chem. Soc.*, **1963**, 3286.
26) W. P. Griffith, J. Lewis, and G. Wilkinson, *ibid.*, **1959**, 872.
27) M. Mori, S. Ueshiba, and S. Kawaguchi, This Bulletin, **36**, 796 (1963).
28) H. Kobayashi, M. Shimizu, and I. Fujita, *ibid.*, **43**, 2335 (1970).
29) A. D. Buckingham and P. J. Stephens, *Ann. Rev. Phys. Chem.*, **7**, 399 (1966).
30) P. J. Stephens, *J. Chem. Phys.*, **52**, 3489 (1970).
31) The conventional molar ellipticity per unit external magnetic field $[\theta]_M$ is obtained by 3300 $(\varepsilon_l-\varepsilon_r)/H_z$.
32) S. Koide and M. H. L. Pyrce, *Phil. Mag.*, **3**, 607 (1958).
33) J. S. Griffith, "The Theory of Transition-Metal Ions," Cambridge University Press (1961), p. 302.
34) N. G. Vannerberg, *Acta Chem. Scand.*, **20**, 1571 (1966).
35) W. B. Lewis and L. O. Morgan, "Transition Metal Chemistry" Vol. IV, ed. by R. L. Carlin, M. Dekker New York (1968), p. 67.